

MIT Open Access Articles

Lattice-Imposed Geometry in Metal-Organic Frameworks: Lacunary Zn₄₀ Clusters in MOF-5 Serve as Tripodal Chelating Ligands for Ni²⁺

The MIT Faculty has made this article openly available. **Please share** how this access benefits you. Your story matters.

Citation: Brozek, Carl K., and Mircea Dincă. "Lattice-imposed Geometry in Metal-organic Frameworks: Lacunary Zn₄₀ Clusters in MOF-5 Serve as Tripodal Chelating Ligands for Ni²⁺." *Chemical Science* 3.6 (2012): 2110.

As Published: <http://dx.doi.org/10.1039/C2SC20306E>

Publisher: Royal Society of Chemistry, The

Persistent URL: <http://hdl.handle.net/1721.1/78285>

Version: Author's final manuscript: final author's manuscript post peer review, without publisher's formatting or copy editing

Terms of use: Creative Commons Attribution-Noncommercial-Share Alike 3.0



Cite this: DOI: 10.1039/c0xx00000x

www.rsc.org/xxxxxx

Lattice-Imposed Geometry in Metal-Organic Frameworks: Lacunary Zn_4O Clusters in MOF-5 Serve as Tripodal Chelating Ligands for Ni^{2+}

Carl K. Brozek and Mircea Dincă*

Received (in XXX, XXX) Xth XXXXXXXXX 20XX, Accepted Xth XXXXXXXXX 20XX

DOI: 10.1039/b000000x

The inorganic clusters in metal-organic frameworks can be used to trap metal ions in coordination geometries that are difficult to achieve in molecular chemistry. We illustrate this concept by using the well-known basic carboxylate clusters in $Zn_4O(1,4\text{-benzenedicarboxylate})_3$ (MOF-5) as tripodal chelating ligands that enforce an unusual pseudo-tetrahedral oxygen ligand field around Ni^{2+} . The new Ni-based MOF-5 analogue is characterized by porosity measurements and a suite of electronic structure spectroscopies. Classical ligand field analysis of the Ni^{2+} ion isolated in MOF-5 classifies the $Zn_3O(\text{carboxylate})_6$ "tripodal ligand" as an unusual, stronger field ligand than halides and other oxygen donor ligands. These results may inspire the wide-spread usage of MOFs as chelating ligands for stabilizing site-isolated metal ions in future reactivity and electronic structure studies.

The ability to tune the electronic properties of a metal ion by changing its coordination environment is the cornerstone of transition-metal chemistry. The design of ligands that enforce desired geometries around metals is the typical approach towards this goal and has been the purview of a molecular science; such tunability in the solid state is rare. With an eye towards the latter, we sought to use the inorganic clusters in metal-organic frameworks (MOFs), a class of porous crystalline materials made from simple building blocks, as chelating ligands. Although coordinatively unsaturated metal ions with unusual geometries have been isolated in MOFs in the context of gas storage and separation or catalysis,¹ the deliberate use of MOF nodes in coordination chemistry remains virtually unexplored. As a proof-of-principle, we reconceived the secondary building unit (SBU) of the iconic $Zn_4O(\text{BDC})_3$ (MOF-5, BDC = 1,4-benzenedicarboxylate)² as a tripodal ligand for metals that are typically incompatible with tetrahedral oxygen ligand fields, such as Ni^{2+} (see Figure 1). Normally, Ni^{2+} (d^8) prefers octahedral coordination in oxygen ligand fields and assumes tetrahedral geometry only when trapped in condensed lattices such as ZnO ,³ or when surrounded by bulky supporting ligands.⁴ By demonstrating that the $Zn_4O(\text{carboxylate})_6$ SBU can be used as a designer chelating ligand we hope to inspire the use of these popular materials as platforms for unusual coordination chemistry.

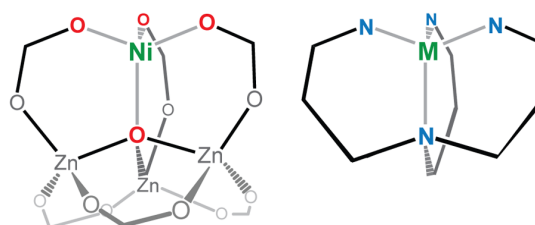


Fig. 1 Illustration of the $Zn_3O(\text{carboxylate})_6$ SBU of MOF-5 as a tripodal support that enforces a tetrahedral oxygen ligand field, akin to standard chelating ligands such as the tetra-amine on the right.

Our first attempts to install Ni^{2+} ions inside MOF-5 were inspired by isolated reports of post-synthetic ion metathesis at MOF nodes.⁵ Complete metathesis of structural units is a powerful method to access rationally designed analogues of existing MOFs, as has recently also been demonstrated by organic ligand exchange.⁶ Accordingly, colourless crystals of MOF-5 were soaked in a saturated solution of $Ni(\text{NO}_3)_2 \cdot 6\text{H}_2\text{O}$

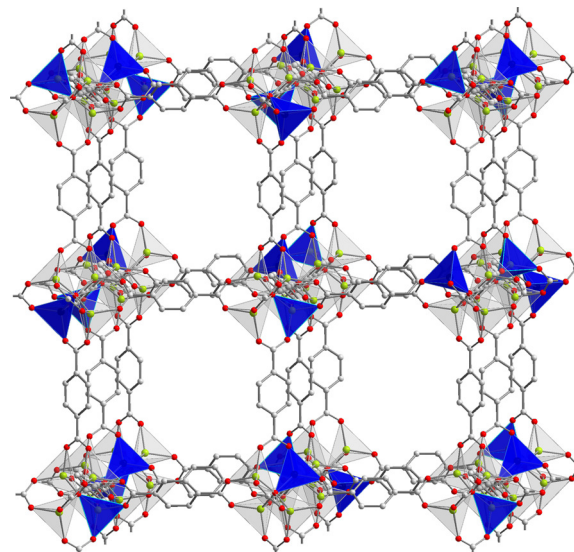


Fig. 2 Part of the crystal structure of $Ni_xZn_{4-x}O(\text{BDC})_3$ ($x = 1$). Due to crystallographically-imposed symmetry, the position of Ni^{2+} centers (blue tetrahedra) within individual $NiZn_3$ clusters cannot be identified unambiguously, and these are depicted at random. Green, red, and grey spheres represent Zn, O, and C atoms, respectively. Hydrogen atoms are omitted for clarity.

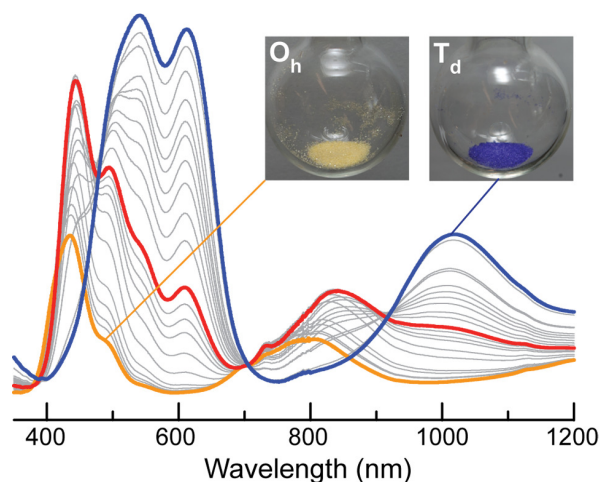


Fig. 3 In-situ diffuse-reflectance spectra depicting the color progression from yellow **(DMF)₂Ni-MOF-5** to blue **Ni-MOF-5** via a putative pentacoordinated Ni²⁺ intermediate (red trace). The inset shows optical images of the yellow and blue crystals.

and, to our satisfaction, turned yellow within a few days. To ensure maximal Ni²⁺ incorporation, soaking was continued for one year. The ensuing yellow crystals were washed repeatedly with *N,N*-dimethylformamide (DMF) and CH₂Cl₂ without loss of colour until the solvents no longer showed UV-Vis absorption profiles characteristic of free Ni²⁺ ions. X-ray diffraction and elemental analysis of these yellow crystals revealed a cubic lattice ($a = 25.838(2) \text{ \AA}$) nearly identical to that of MOF-5 and a Ni:Zn ratio of 1:3. Shorter soaking times engendered lower levels of Ni²⁺ substitution, and Ni:Zn ratios of 1:10 could be isolated after two weeks. Albeit slow, these results indicated that spontaneous substitution of Ni²⁺ into MOF-5 is thermodynamically favourable and suggested that Ni²⁺-substituted MOF-5 may also be accessible by direct synthesis. Indeed, heating mixtures of Zn(NO₃)₂•6H₂O, Ni(NO₃)₂•6H₂O, and H₂BDC in DMF afforded cubic yellow crystals whose diffraction pattern matched that of MOF-5. As expected for a kinetically controlled process, the Ni:Zn ratio in these samples depended on the relative concentrations of Ni(NO₃)₂•6H₂O and Zn(NO₃)₂•6H₂O yet never exceeded 1:3 (Figure S2). In fact, increasing the Ni:Zn ratio in the reactant mixture above 6:1 led to selective formation of a yet unidentified crystalline green powder that did not match the X-ray diffraction pattern of any known Ni²⁺-BDC or Zn²⁺-BDC phases.⁷ The upper limit of the Ni²⁺ content was similar to what had previously been reported as a curiosity in Co²⁺-substituted MOF-5 materials.⁸

We herein provide a hypothesis for this surprising observation: the yellow colour of as-synthesized Ni²⁺-substituted MOF-5 is indicative of *octahedral* Ni²⁺. We surmise that accommodation of octahedral Ni²⁺ must distort the original Zn₄O core and the MOF-5 lattice. Additional Ni²⁺ substitution into the ensuing NiZn₃O cluster is prevented by a large kinetic barrier as it would exert debilitating strain on the lattice. The presence and identity of the two additional ligands that complete the coordination sphere of octahedral Ni²⁺ was confirmed by thermogravimetric analysis, which showed that two DMF molecules per Ni centre are lost by heating the yellow crystals between 70 and 150 °C (Figure S3). Zn₄O(carboxylate)₆ SBUs wherein one Zn²⁺ is hexa-coordinate

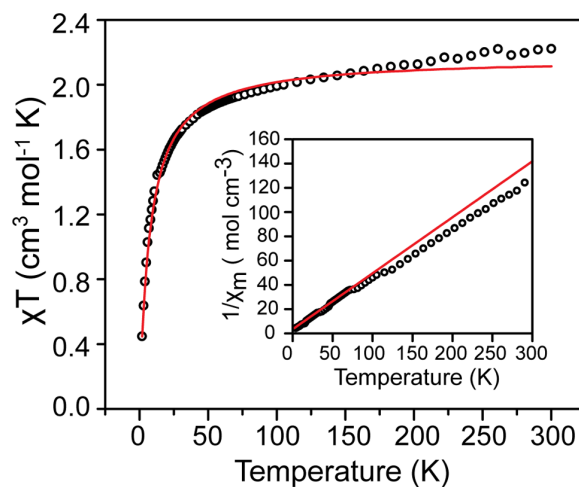


Fig. 4 The temperature dependence of $\chi_m T$ of evacuated **Ni-MOF-5** (circles). The red trace represents a fit obtained using julX.17^{17} We note that the observed temperature dependence of $\chi_m T$ is due to thermally accessible multiplet states of the ${}^3T_1(F)$ ground state, and not antiferromagnetic coupling. This is confirmed by a nearly (0,0) intercept of the Curie-Weiss plot (inset).

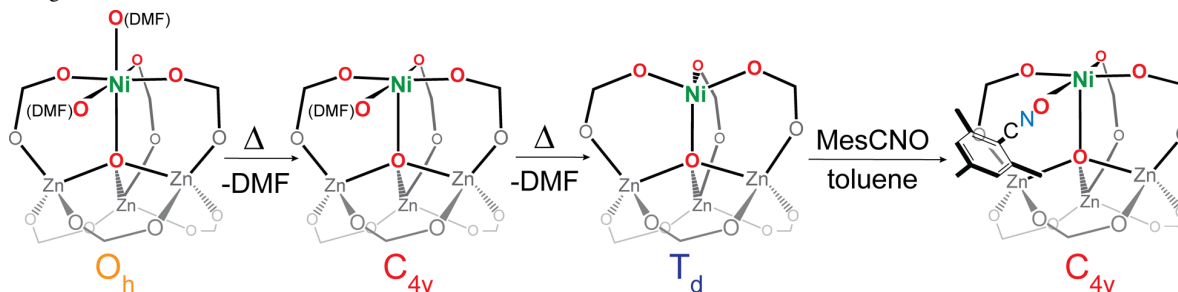
and binds two DMF molecules have been reported,⁹ offering precedent for the formulation of Ni-substituted MOF-5 as **(DMF)_{2x}Ni_xZn_{4-x}O(BDC)₃** ($0 < x < 1$), **(DMF)₂Ni-MOF-5**.¹⁰

Table 1 Calculated Racah and ligand field parameters of various tetrahedral Ni²⁺ species based on observed transitions ν_2 and ν_3 .

Species	ν_3 (cm ⁻¹)	ν_2 (cm ⁻¹)	B (cm ⁻¹)	Dq (cm ⁻¹)
¹¹ [Ni(NCO) ₄] ²⁻	16200	9460	511	311
¹¹ [NiCl ₄] ²⁻	14760	7470	405	206
¹¹ [NiBr ₄] ²⁻	13320	6995	379	201
^{4d} [Ni(OAr) ₄] ²⁻	16820	10000	867	540
^{3a} ZnO:Ni ²⁺	15720	8340	770	420
^{3a} ZnS:Ni ²⁺	12790	9750	560	475
^{3a} CdS:Ni ²⁺	12395	7840	570	400
Ni-MOF-5	17406	9803	1045	753

Remarkably, heating **(DMF)₂Ni-MOF-5** under vacuum afforded deep blue-purple crystals of Ni_xZn_{4-x}O(BDC)₃ (**Ni-MOF-5**), a new analogue of MOF-5 that contains pseudo-tetrahedral Ni²⁺ supported only by oxygen ligands, shown in Figure 2. Single crystal X-ray diffraction analysis revealed that the asymmetric unit of **Ni-MOF-5** contains a single metal site, indicating that Ni²⁺ substitutes Zn²⁺ inside the SBU of a structure otherwise identical to MOF-5. Functional similarity to MOF-5 was also established by porosity measurements: blue **Ni-MOF-5** adsorbed 825 cm³ of N₂/g at 1 atm and 77 K and exhibited a BET surface area of 3300(100) m²/g, analogous to original MOF-5 (Figure S9).¹² FT-IR analysis of **Ni-MOF-5** confirmed the absence of a C=O stretch at 1660 cm⁻¹ that would be expected if DMF were still coordinated to Ni²⁺ (Figure S4). In contrast to Be²⁺ and Co²⁺ analogues of MOF-5,¹³ **Ni-MOF-5** is built from SBUs that do not have molecular analogues, highlighting the importance of the lattice in stabilizing otherwise inaccessible molecular species. Soaking basic zinc acetate crystals,

Scheme 1 Sequential loss of DMF molecules from a $(\text{DMF})_2\text{NiZn}_3\text{O}(\text{carboxylate})_6$ cluster and isolation of a MesCNO adduct. Symmetry labels indicate the idealized geometries at the Ni^{2+} centers.



$\text{Zn}_4\text{O}(\text{O}_2\text{C}-\text{CH}_3)_6$,¹⁴ in an anhydrous DMF solution of $\text{Ni}(\text{NO}_3)_2 \cdot 6\text{H}_2\text{O}$ for up to three weeks led to the decomposition of the metal cluster, not the incorporation of Ni^{2+} . Therefore, $\text{NiZn}_3\text{O}(\text{carboxylate})_6$ clusters can only be stabilized in the MOF

5 lattice. The pseudo-tetrahedral geometry around the Ni^{2+} and the homogeneity of **Ni-MOF-5** was quantified by diffuse-reflectance UV-Vis-NIR spectroscopy (blue trace in Figure 3), and magnetic measurements (vide infra). Despite the slight deviation from tetrahedral geometry around Ni^{2+} , **Ni-MOF-5** exhibited a spectrum that resembled solution-phase spectra of strictly tetrahedral Ni^{2+} complexes.¹⁵ Thus, a peak at 1020 nm (9803 cm^{-1}) can be assigned to the ${}^3\text{T}_1(\text{F}) - {}^3\text{A}_2$ transition of a d^8 tetrahedral ion (ν_2), while the doublet of peaks at 540 nm (18,500 cm^{-1}) and 608 nm (16,400 cm^{-1}) can be assigned to the ${}^3\text{T}_1(\text{F}) - {}^3\text{T}_1(\text{P})$ transition (ν_3), where ${}^3\text{P}$ is split by spin-orbit coupling into ${}^3\text{P}_0$ (A_1), ${}^3\text{P}_1$ (T_1), ${}^3\text{P}_2$ ($\text{E}+\text{T}_2$) respectively.^{3a} A ligand field analysis of this spectrum using a system of equations originally derived by Ballhausen^{15g} (see Supporting Information) revealed Racah and Dq parameters of 1045 cm^{-1} and 753 cm^{-1} . As shown in Table 1, these are notably higher than those common for tetrahedral Ni^{2+} and suggest that spin-spin repulsion is almost as large as in unperturbed Ni^{2+} ions, thereby preserving a large spin-orbit coupling interaction.

25 The presence of significant spin-orbit coupling was also evidenced by magnetic measurements. A $\chi_m T$ vs. T plot of **Ni-MOF-5**, shown in Figure 4, revealed the presence of magnetically dilute Ni^{2+} ions and a room temperature magnetic moment of 4.21 μ_B per Ni^{2+} ion. This value is higher than the spin-only value expected for Ni^{2+} , but is expected for tetrahedral d^8 ions subject to unquenched orbital angular momentum.¹⁶ The value of μ_{eff} is further elevated by a temperature independent paramagnetism value of $0.2 \times 10^{-6} \text{ cm}^3/\text{mol}$ as determined by a fit of the susceptibility data using julX .¹⁷

35 Hints at the reactivity of Ni^{2+} centers within **Ni-MOF-5** came from an in-situ UV-Vis-NIR study of the striking color change that occurs when heating **(DMF)₂Ni-MOF-5**. These experiments, plotted in Figure 3, evidenced an isosbestic point around 700 nm, which suggested that DMF loss occurred in two kinetically independent processes via a well-defined five-coordinate Ni^{2+} species. The identity of this species was probed by treating **Ni-MOF-5** with various nucleophiles. Although the reaction of **Ni-MOF-5** with small ligands such as PMe_3 , THF, and MeCN rapidly produced octahedral Ni^{2+} , indicated by a color reversal to yellow, sterically-demanding MesCNO afforded an orange adduct, whose spectrum matched that of the putative

pentacoordinate **(DMF)Ni-MOF-5** adduct (Figure S5). Thus, Figure 3 shows a straightforward six- (O_h) to five- (C_{4v}) to four- (pseudo- T_d) coordinate conversion of Ni in a +2 formal oxidation state. These transformations, illustrated in Scheme 1, are supported by computational modeling of $(\text{DMF})_y\text{NiZn}_3\text{O}(\text{benzoate})_6$ ($y = 0, 1, 2$) clusters containing six-, five-, and four-coordinate Ni^{2+} ions with two, one, or no bound DMF molecules. As shown in Figure S7, time-dependent DFT calculations using optimized geometries of these clusters predicted electronic absorption spectra that agreed well with the assigned yellow, red, and blue traces in Figure 3.

Conclusions

The use of the inorganic nodes in MOF-5 as unusual chelating ligands illustrates a potentially rich area of exploration in coordination chemistry. Extending this concept to other metals and MOF systems will enable synthetic inorganic chemists to pursue a variety of important goals, including the isolation of "hot" intermediates from industrial and biological catalytic processes.

Acknowledgements

This work was supported by the U.S. Department of Energy, Office of Science, Office of Basic Energy Sciences under Award Number DE-SC0006937. Grants from the NSF provided instrument support to the DCIF at MIT (CHE-9808061, DBI-9729592). This work made use of the MRSEC Shared Experimental Facilities at MIT, supported in part by the NSF under award number DMR-0819762. We thank Dr. Natalia Shustova for assistance with refinement of the X-ray crystal structure and Dr. Anthony Cozzolino for assistance with performing computations in ORCA. CKB acknowledges graduate tuition support from the NSF.

Notes and references

Department of Chemistry, Massachusetts Institute of Technology, 77 Massachusetts Avenue, Cambridge, MA, 02139-4307. Email: mindca@mit.edu

† Electronic Supplementary Information (ESI) available: Experimental procedures, X-ray structure refinement tables and details, computational details, relevant equations for LF analysis, powder X-ray diffraction patterns, ICP-AES results, TGA, FT-IR spectra, additional diffuse reflectance spectra, calculated electronic transitions, and an N_2 isotherm plot and data table. See DOI: 10.1039/b000000x/

- ¹ (a) S. S.-Y. Chui, S. S. H. Lo, J. P. H. Charmant, A. G. Orpen, I. D. Williams, *Science*, 1999, **283**, 1148. (b) B. Chen, M. Eddaoudi, T. M. Reineke, J. W. Kampf, M. O'Keefe, O. M. Yaghi, *J. Am. Chem. Soc.*, 2000, **122**, 11559. (c) N. L. Rosi, J. Kim, M. Eddaoudi, B. Chen, M. O'Keefe, O. M. Yaghi, *J. Am. Chem. Soc.*, 2005, **127**, 1504. (d) P. D. C. Dietzel, Y. Morita, R. Blom, H. Fjellvåg, *Angew. Chem. Int. Ed.*, 2005, **44**, 6354. (e) A. Vimont, J. M. Goupil, J. C. Lavalley, M. Daturi, S. Surblé, C. Serre, F. Millange, G. Férey, N. Audebrand, *J. Am. Chem. Soc.*, 2006, **128**, 3218. (f) P. M. Forster, J. Eckert, B. D. Heiken, J. B. Parise, J. W. Yoon, S. H. Jhung, J. S. Chang, A. K. Cheetham, *J. Am. Chem. Soc.*, 2006, **128**, 16846. (g) M. Dincă, A. Dailly, Y. Liu, C. M. Brown, D. A. Neumann, J. R. Long, *J. Am. Chem. Soc.*, 2006, **128**, 16876. (h) S. Ma, H. C. Zhou, *J. Am. Chem. Soc.* 2006, **128**, 11734. (i) O. K. Farha, A. M. Spokoyny, K. L. Mulfort, M. F. Hawthorne, C. A. Mirkin, J. T. Hupp, *J. Am. Chem. Soc.* 2007, **129**, 12680. (j) M. Dincă, J. R. Long, *Angew. Chem. Int. Ed.*, 2008, **47**, 6766. (k) S. R. Caskey, A. G. Wong-Foy, A. J. Matzger, *J. Am. Chem. Soc.*, 2008, **130**, 10870. (l) L. J. Murray, M. Dincă, J. Yano, S. Chavan, S. Bordiga, C. M. Brown, J. R. Long, *J. Am. Chem. Soc.*, 2010, **132**, 7856. (m) E. D. Bloch, L. M. Murray, W. L. Queen, S. Chavan, S. N. Maximoff, J. P. Bigi, R. Krishna, V. K. Peterson, F. Grandjean, G. J. Long, B. Smith, S. Bordiga, C. M. Brown, J. R. Long, *J. Am. Chem. Soc.*, 2011, **133**, 14814.
- ² H. Li, M. Eddaoudi, M. O'Keefe, O. M. Yaghi, *Nature*, 1999, **402**, 276.
- ³ (a) H. A. Weakliem, *J. Chem. Phys.*, 1962, **36**, 2117. (b) D. A. Schwartz, N. S. Norberg, Q. P. Nguyen, J. M. Parker, D. R. Gamelin, *J. Am. Chem. Soc.*, 2003, **125**, 13205.
- ⁴ (a) X. B. Cui, S. T. Zheng, G. Y. Yang, *Z. Anorg. Allg. Chem.*, 2005, **631**, 642. (b) J. W. Zhao, H. P. Jia, J. Zhang, S. T. Zheng, G. Y. Yang, *Chem.-Eur. J.* 2007, **13**, 10030. (c) G. G. Gao, L. Xu, W. J. Wang, X. S. Qu, H. Liu, Y. Y. Yang, *Inorg. Chem.*, 2008, **47**, 2325. (d) B. Zheng, M. O. Miranda, A. G. DePasquale, J. A. Golen, A. L. Rheingold, L. H. Doerrer, *Inorg. Chem.*, 2009, **48**, 4272. (e) P. R. Ma, D. Q. Bi, J. P. Wange, W. Wang, J. Y. Niu, *Inorg. Chem. Commun.* 2009, **12**, 1182.
- ⁵ (a) M. Dincă, J. R. Long, *J. Am. Chem. Soc.*, 2007, **129**, 11172. (b) L. Mi, H. Hou, Z. Song, H. Han, H. Xu, Y. Fan, S. W. Ng, *Cryst. Eng. Design.* 2007, **7**, 2553. (c) L. Mi, H. Hou, Z. Song, H. Han, Y. Fan, *Chem. Eur. J.*, 2008, **14**, 1814. (d) J. Zhao, L. Mi, J. H. Hou, Y. Fan, *J. Am. Chem. Soc.*, 2008, **130**, 15222. (e) S. Das, H. Kim, K. Kim, *J. Am. Chem. Soc.*, 2008, **130**, 3814. (f) J. Li, L. Li, H. Hou, Y. Fan, *Cryst. Growth Des.* 2009, **9**, 4504. (g) T. K. Prasad, D. H. Hong, M. P. Suh, *Chem. Eur. J.*, 2010, **16**, 14043. (h) S. Huang, X. Li, X. Shi, H. Hou, Y. Fan, *J. Mater. Chem.* 2010, **20**, 5695. (i) A. D. Burrows, *Cryst. Eng. Comm.*, 2011, **13**, 3623. (j) Z. Zhang, L. Zhang, L. Wojtas, P. Nugent, M. Eddaoudi, M. J. Zaworotko, *J. Am. Chem. Soc.*, 2011, **134**, 924.
- ⁶ M. Kim, J. F. Cahill, Y. Su, K. A. Prather, S. M. Cohen, *Chem. Sci.* 2012, **3**, 126.
- ⁷ Repeated attempts to grow single crystals of this Ni²⁺-BDC phase were not successful. A search of the Cambridge Crystallographic Database indicated, to our surprise, that no pure Ni²⁺-BDC MOF has been reported so far (i.e. containing no other chelating/bridging ligands).
- ⁸ J. A. Botas, G. Calleja, M. Sánchez-Sánchez, M. G. Orcajo, *Langmuir*, 2010, **26**, 5300.
- ⁹ B. Kesanli, Y. Cui, M. R. Smith, E. W. Bittner, B. C. Bockrath, W. Lin, *Angew. Chem. Int. Ed.*, 2005, **44**, 72.
- ¹⁰ Accordingly, we propose that the materials reported in reference 6 may also be formulated as (DMF)_{2x}Co_xZn_{4-x}O(BDC)₃.
- ¹¹ A. B. P. Lever, *Inorganic Electronic Spectroscopy*; Elsevier: New York, 1984; p. 864.
- ¹² S. S. Kaye, A. Dailly, O. M. Yaghi, J. R. Long, *J. Am. Chem. Soc.*, 2007, **129**, 14176.
- ¹³ S. Hausdorf, F. Baitalow, T. Bohle, D. Rafaja, F. O. R. L. Mertens, *J. Am. Chem. Soc.*, 2010, **132**, 10978.
- ¹⁴ R. M. Gordon, H. B. Silver, *Can. J. Chem.*, 1983, **61**, 1218.
- ¹⁵ (a) B. R. Sundheim, G. Harrington, *J. Chem. Phys.*, 1959, **31**, 700. (b) D. M. Gruen, R. L. McBeth, *J. Phys. Chem.*, 1959, **63**, 393. (c) N. S. Gill, R. S. Nyholm, *J. Chem. Soc.*, 1959, 3997. (d) A. D. Liehr, C. Ballhausen, *J. Ann. Phys.*, 1959, **2**, 134. (e) C. Furlani, G. Morpurgo, *Z. Physik. Chem.*, 1961, **28**, 93. (f) D. M. L. Goodgame, M. Goodgame, F. A. Cotton, *J. Am. Chem. Soc.*, 1961, **83**, 4161. (g) C. Ballhausen, *J. Adv. Chem. Phys.*, 1963, **5**, 33.
- ¹⁶ (a) B. N. Figgis, *Nature*, 1958, **182**, 1568. (b) B. N. Figgis, J. Lewis, F. Mabbs, G. A. Webb, *Nature*, 1964, **203**, 1138. (c) B. N. Figgis, J. Lewis, F. E. Mabbs, G. A. Webb, *J. Chem. Soc. (A)*, 1966, 1412.
- ¹⁷ http://ewww.mpi-muelheim.mpg.de/bac/logins/bill/julX_en.php